Second order diffraction forces on a vertical cylinder in regular waves

R. EATOCK TAYLOR and S. M. HUNG

London Centre for Marine Technology, University College London, Torrington Place, London WC1E 7JE

INTRODUCTION

The evaluation of wave forces on vertical surface piercing cylinders has been a subject of interest for over 40 years, since Havelock[1] first published the analysis of first order diffraction in infinite water depth. In the extension of the analysis to second order forces, contributions due to a second order velocity potential must be accounted for, in addition to those from the first order potential. Hitherto the solution for the second order potential has been fraught with difficulties and controversies. To our knowledge, a correct method for general solution in three dimensions, satisfying all the boundary conditions, has not yet been published. One can cite, for instance, a recent study of axisymmetric bodies by Sabuncu and Goren,[2] in which a general solution was used that satisfies neither the free surface boundary condition nor the radiation boundary condition at large distance.

In many applications it is the second order forces on a body that are of interest, rather than the second order potential at a point in the fluid. Various authors have therefore suggested a methodology for obtaining forces without explicitly evaluating the second order potential. Through the use of Green's second identity, the forces are expressed in terms of first order potentials alone. The resulting expressions for infinite water depth were given by Lighthill,[3] and Molin[4] has presented the results for finite water depth. Unfortunately, however, these formulations involve a free surface integral, for which a converged solution has hitherto been extremely difficult to obtain. In practice it is necessary to make certain assumptions about the behaviour of the second order potential at a large distance from the body, but these have not been clearly assessed.

In the study reported here, we have set out to re-examine the theory given by Lighthill and Molin, and to derive definitive results. In several respects, our formulation is very similar to that given by Molin and Marion,[5] in a report which came to our attention during the course of our investigations. In order to justify the omission of certain terms when Green's identity is invoked, we have attempted to give special consideration to the far field behaviour of the second order scattered potential; and although our conclusions are the same, our arguments in this respect are somewhat different from those of Molin and Marion. Our solution also differs in that we have used our knowledge of the far field behaviour of the first and second order potential in order to obtain a converged solution to the awkward free surface integral. This part of our solution makes use of asymptotic forms which have also been used by Matsui.[6]

In the following, we present analytical expressions for the second order force on a vertical surface piercing cylinder. Except for the aforementioned contribution from the free surface integral, these expressions confirm those given by Molin and Marion. Our numerical results agree, for the cases where we have made comparisons, thereby providing independent confirmation of the evaluation of the free surface integral (which is found to make a very significant contribution). Additionally, results for infinite water depth are also derived and compared with those given by Lighthill[3] and Hunt and Baddour.[7]

Based on the formulations presented in this paper, it is envisaged that an accurate and economical solution of forces for general three dimensional bodies in regular or bichromatic waves will also become a possibility.

MATHEMATICAL PRELIMINARIES

We define a polar co-ordinate system $O_{r\theta z}$ (Fig. 1), such that the z axis points vertically upwards, with $O_{r\theta}$ on the mean free surface. With the assumption of irrotational flow, the wave field may be defined by a velocity potential Φ, expressible in the form of the Stokes expansion:

$$\Phi = \Phi^{(1)} + \Phi^{(2)} \tag{1}$$

This series implies a perturbation parameter proportional to wave steepness. The first order velocity potential for a regular wave of frequency ω is:

$$\Phi^{(1)} = \mathrm{Re}\,[\phi^{(1)} e^{i\omega t}] \tag{2}$$

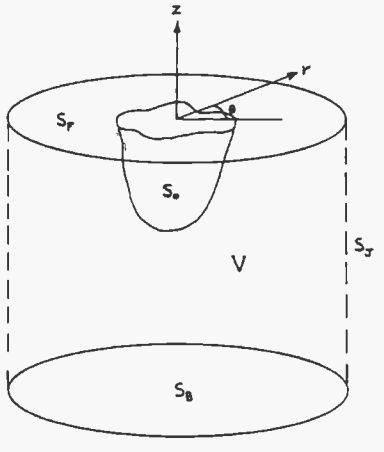

Figure 7. Definition of geometry

Accepted May 1986. Discussion closes March 1987.

0141-1187/87/010019-12 $2.00

which can be decomposed into incident and scattered components:

$$\Phi^{(1)} = \Phi_I^{(1)} + \Phi_S^{(1)} \tag{3}$$

In the fluid region V

$$\nabla^2 \Phi^{(1)} = 0 \tag{4}$$

on the body surface S_0 and sea bed S_B

$$\frac{\partial \Phi^{(1)}}{\partial n} = 0 \tag{5}$$

and on the mean free surface S_F

$$\frac{\partial^2 \Phi^{(1)}}{\partial t^2} + g \frac{\partial \Phi^{(1)}}{\partial z} = 0 \tag{6}$$

In addition, $\Phi_S^{(1)}$ must satisfy the Sommerfeld radiation boundary condition:

$$\lim_{r \to \infty} \sqrt{r} \left(\frac{\partial \Phi_S^{(1)}}{\partial r} + ik \Phi_S^{(1)} \right) = 0 \tag{7}$$

where for water depth d the wave number k satisfies:

$$\frac{\omega^2}{g} = k \tanh kd \tag{8}$$

For an incident wave of amplitude A travelling in the direction $\theta = 0$,

$$\phi_I^{(1)} = \frac{gA}{\omega} \frac{\cosh k(z+d)}{\cosh kd} e^{-ikr\cos\theta} \tag{9}$$

The wave elevation $\Xi^{(1)}$ is defined by

$$\Xi^{(1)} = -\frac{1}{g} \frac{\partial \Phi^{(1)}}{\partial t} \quad \text{on } S_F \tag{10}$$

Therefore

$$\Xi^{(1)} = \mathrm{Re}\,[\xi^{(1)} e^{i\omega t}] \tag{11}$$

where

$$\xi^{(1)} = -\frac{i\omega}{g} \phi^{(1)} \tag{12}$$

The associated second order velocity potential is defined by

$$\Phi^{(2)} = \Phi_I^{(2)} + \Phi_S^{(2)} \tag{13}$$

$$= \mathrm{Re}\,[\phi^{(2)} e^{i2\omega t} + \delta^{(2)} t] \tag{14}$$

where

$$\nabla^2 \Phi^{(2)} = 0 \quad \text{in } V \tag{15}$$

$$\frac{\partial \Phi^{(2)}}{\partial n} = 0 \quad \text{on } S_0 \cup S_B \tag{16}$$

$$\frac{\partial^2 \Phi^{(2)}}{\partial t^2} + g \frac{\partial \Phi^{(2)}}{\partial z} = -\frac{\partial}{\partial t}[(\nabla\Phi)^2] + \frac{1}{g} \frac{\partial \Phi^{(1)}}{\partial t} \left[\frac{\partial}{\partial z} \left(\frac{\partial^2 \Phi^{(1)}}{\partial t^2} + g \frac{\partial \Phi^{(1)}}{\partial z} \right) \right] \quad \text{on } S_F \tag{17}$$

The second order radiation boundary condition is as yet undefined, but will be discussed later. The second order complex incident potential $\phi_I^{(2)}$ may be obtained by substituting equation (9) into the right hand side of equation (17), yielding

$$\phi_I^{(2)} = -\frac{i3A^2\omega}{8} \frac{\cosh 2k(z+d)}{\sinh^4 kd} e^{-i2kr\cos\theta} \tag{18}$$

The second order wave elevation $\Xi^{(2)}$ is given by

$$\Xi^{(2)} = -\frac{1}{g} \left[\frac{\partial \Phi^{(2)}}{\partial t} + \frac{1}{2} (\nabla \Phi^{(1)})^2 - \frac{1}{g} \frac{\partial \Phi^{(1)}}{\partial t} \frac{\partial^2 \Phi^{(1)}}{\partial z\, \partial t} \right] \tag{19}$$

Substituting equation (9) into the last two terms of equation (19), we obtain the value of $\delta_I^{(2)}$ which causes $\Xi^{(2)}$ to oscillate about the mean free surface in an otherwise undisturbed incident wave:

$$\delta_I^{(2)} = -\frac{A^2 gk}{2 \sinh 2kd} \tag{20}$$

We comment here that on physical grounds $\delta^{(2)}$ must be spatially independent, and therefore it does not contribute to horizontal forces on the body up to second order.[8]

HYDRODYNAMIC FORCES

General formulation

The first-order horizontal force on a fixed body in direction β is

$$F^{(1)} = -\rho \int_{S_0} \frac{\partial \Phi^{(1)}}{\partial t} n_\beta \, dS \tag{21}$$

where n_β is the component of the unit normal into the body in the direction of β. By retaining terms of second order in the integrated hydrodynamic pressure, the second order force is found to be

$$F^{(2)} = -\rho \left[\int_{z=0} -\frac{g}{2} (\Xi^{(1)})^2 n_\beta \, dl + \frac{1}{2} \int_{S_0} (\nabla \Phi^{(1)})^2 n_\beta \, dS + \int_{S_0} \frac{\partial \Phi^{(2)}}{\partial t} n_\beta \, dS \right] \tag{22}$$

where $\int_{z=0} dl$ denotes an integral at the water line, and the body is assumed to intersect the free surface vertically.

The first two terms of equation (22) can be decomposed into a mean ($F_m^{(2)}$) and time oscillatory component ($F_0^{(2)}$) respectively, such that

$$F_m^{(2)} = \mathrm{Re} \left[\frac{\rho g}{4} \int_{z=0} \xi^{(1)} \cdot \xi^{(1)*} n_\beta \, dl - \frac{\rho}{4} \int_{S_0} \nabla \phi^{(1)} \cdot \nabla \phi^{(1)*} n_\beta \, dS \right] \tag{23}$$

$$F_0^{(2)} = \mathrm{Re} \left[\left\{ \frac{\rho g}{4} \int_{z=0} \xi^{(1)} \cdot \xi^{(1)} n_\beta \, dl - \frac{\rho}{4} \int_{S_0} \nabla \phi^{(1)} \cdot \nabla \phi^{(1)} n_\beta \, dS \right\} e^{i2\omega t} \right] \tag{24}$$

ives to eq. (9). The results are similar to eq. (4) and eq. (5), with the addition of the free surface integral over S_F which we have included in eq. (9). In this case ν in eq. (4) takes the value Ω_2^2/g.

3. NUMERICAL SCHEMES

By far the commonest method of solving integral equations such as eq. (1) or eq. (2) for the radiation and diffraction problems is the constant panel method. In this, the velocity is generally assumed constant over a flat panel, and the integral equation is enforced at a representative point on each panel, usually the centroid. The approach has its origins in earlier work in the field of aerodynamics (eg Hess and Smith 1964). Early examples of its application to offshore structures were given by Hogben and Standing (1974) and others. Since then, with developments in computing, it has become possible to apply this approach to complex structures idealised by large numbers of panels, as for example the TLP discretised by Korsmeyer et al (1988) using up to 12,608 panels (or 3152 per quadrant, with double symmetry).

Features of the constant panel method are that curved surfaces are represented by multi-faceted models, which may have discontininties (hence "leaks"); and the distribution of potential (or source strength) is discontinuous. One would assume that with a well formulated method such discontinuites become of decreasing importance, as increasing computing power facilitates the use of increasingly fine discretisations. Doubts, however, have been expressed by Liu, Kim and Lu (1990) concerning the convergence of the constant panel method for bodies with sharp corners. They argue that the limit of the constant C in eq. (1), when evaluated at the centroid of panels of ever decreasing size, does not tend to the value of C associated with the solid angle of the corner itself. The relevance of this assertion is currently unclear, both numerically and in relation to the modelling of unseparated flow at sharp corners.

One may also legitimately ask whether the constant panel method is indeed the most cost effective method of achieving adequately converged results. Experience with the finite element method, and applications of the boundary integral (or boundary element) method to other fields, suggests that there may be advantages in representing the body surface S_B (and the free surface S_F where necessary) by fewer higher order elements. Indeed there may be greater benefit in the use of higher order boundary elements (where the resulting matrix equations are dense) than in the finite element method (where the coefficient matrix is strongly banded).

The use of quadratic elements to discretise eq. (1) was explored by Eatock Taylor and Zietsman (1982), in the context of a hybrid finite elementboundary integral procedure. In this, the integral equation was in fact written on a fictitious box shaped surface, enclosing a finite element mesh around the body: for this reason many of the contributions to the integral (ie the normal derivatives) were either zero or rather simple to evaluate. More recently quadratic isoparametric elements have been used to discretise the body surface itself: Chau and Eatock Taylor (1988) and Chau 1989 did this in the context of eq. (4); while Liu (1988) and Lui et al (1990) used this idealisation with eq. (1). Others have used higher order elements with simple singularities (e.g. Rankine sources) distributed over the body, free surface, seabed and a radiation boundary. Wu and Eatock Taylor (1989) adopted quadratic isoparametric elements in their solution for the hydrodynamics of translating oscillating bodies: the translating pulsating source was used in the appropriate integral equation expressed over the body surface S_B and the water line (ie the intersection of S_B with the plane z=0). In this case, and in the non-linear diffraction problem involving a free surface integral - c.f. eq. (9) - there is added significance in directly evaluating the water line integral at z=0 (rather than extrapolating from the centroids of constant panels).

An alternative to the direct application of the integral equation at discrete nodal points is to impose the body surface boundary condition in some average sense, for example by variational, Galerkin or weighted residual techniques. This has not received much attention in the context of hydrodynamics, although Breit et al. (1985) used it with the constant panel method for the linear diffraction - radiation problem. The idea may be simply summarised as follows. Suppose we wish to approximate eq. (1), using as discrete unknowns the values of the velocity potential ϕ_j at n nodes (j = 1 to n). In terms of shape functions N_j we can write

$$\phi(x) = \sum_{j=1}^{n} \phi_j N_j(x) \tag{10}$$

In the constant panel method, $N_j(x)$ is simply a surface of unit height over the panel whose centroid is at node j, and zero height elsewhere. For higher order boundary elements, $N_j(x)$ takes the value one at node j, is a varying function over the panels surrounding node j, and is zero elsewhere. The direct application of the boundary integral method reduces eq. (1) in discretised form to the matrix equations

$$A\,\phi = v \tag{11}$$

where

$$A_{ij} = C(x_i)\delta_{ij} + \int_{S_B} \frac{\partial G(x_i;\xi)}{\partial n_\xi} N_j(\xi)\,dS_\xi \tag{12a}$$

$$v_i = \int_{S_B} V(\xi))G(x_i;\xi)\,dS_\xi \tag{12b}$$

To obtain the Galerkin formulation, eq. (1) is multiplied by $N_i(x)$ for each node in term, and integrated over the panels adjacent to node i. The resulting matrix equations are

$$A\,\phi = v \tag{13}$$

where now

$$A_{ij} = \int_{S_B} C(x)N_i(x)N_j(x)\,dS_x + \iint_{S_B S_B} \frac{\partial G(x;\xi)}{\partial n_\xi} N_i(x)N_j(\xi)\,dS_x dS_\xi \tag{14a}$$

$$v_i = \iint_{S_B S_B} V(\xi) G(x;\xi) N_i(x) dS_x dS_\xi \qquad (14b)$$

A particular advantage of using eqs.(13) and (14) is the smoothing of the singularities thereby introduced. This has been illustrated in the context of the ship motion problem by Wu and Eatock Taylor (1989). They describe some of the further advantages in that problem, which involves a water line integral and second derivatives of the steady potential due to forward speed. As the body surface condition on the waterline is averaged over the body surface, in the Galerkin approach, one can avoid the difficulty of the source and field point both lying on the free surface. Furthermore, the second derivatives can be reduced to first derivatives by transforming the Galerkin integral. Similar advantages are apparent in the case of the non-linear diffraction problem.

4. APPLICATION TO THE DIFFRACTION PROBLEM

In the following analysis of the linear and nonlinear diffraction problems, we have used integral equations (4), discretised by quadratic isoparametric elements using equations analogous to eqs. (11) and (12). A number of refinements have been introduced to suppress singularities present in the numerical integrations.

The implementation of the integrals such as those in eq. (12) over generally curved elements requires a transformation to local coordinates. For isoparametric elements this of course involves the same transformation as implied by eq. (10). The resulting integrals over each element must then be evaluated by numerical quadrature. When the field point x_i is not at node j, the kernel, shape functions and Jacobian associated with the isoparametric transformation all remain bounded; Gauss Legendre quadrature may therefore conveniently be employed. A modification, however, is desirable when x_i coincides with node j. This is intended to enhance the accuracy of integrating the modified dipole integral in eq. (4), and to eliminate difficulties arising from singularities associated with the source potentials.

The method adopted here arose from a study of the work by Li et al (1985). They introduced a series of transformations, the effect of which is to reduce the order of singularity of the integrals by one degree, and to allow standard numerical integration to be used over the unit square. The first step is the usual mapping of each boundary element onto a unit square by means of the standard isoparametric transformation. Each square is then subdivided into two or three triangles depending on the location of the singular point. Through the introduction of triangular coordinates, each triangular sub-element is subsequently mapped back onto a unit square (which of course is unrelated to the original unit square before subdivision). A valuable feature of the above sequence of mappings is that they automatically give a great concentration of integration points towards the singular node, and hence Gaussian quadrature of moderate order may be used. This is illustrated in fig. 1, which shows the distribution of integration points produced by the transformation when the singularity is at a mid side node.

To demonstrate the accuracy of the linear diffraction solution acheivable by the procedure, the distribution of the potential $\phi_S^{(1)}$ on the surface of a vertical bottom mounted circular cylinder is presented in table 1. In this case the radius a is equal to the water depth d, and the dimensionless frequency is given by ka=1.4 for a wave number k. The two discretisations shown in fig. 2 were employed, to illustrate convergence. By comparision with the analytical solutions one sees that the numerical results from the finer mesh have essentially converged, and accurate results were obtained from the coarser mesh employing only two elements per quadrant. These results and comparisons of surface tangential velocities and free surface elevations, together with other numerical results for more complex geometries, confirmed the viability of this numerical approach for tackling the second order problem.

Two aspects require special attention in the numerical analysis of the second order problem. One is the efficient calculation of the free surface integral (eg. the third term in eq. (9)), which decays slowly to infinity in a highly oscillatory manner. The other is the need for accurate evaluation of second derivatives of the first order potentials, which also appear in the integral over S_F.

In the present study, the free surface is divided into two regions in which the integrals are treated differently. The inner region, denoted by S_{Fi}, is bounded by the waterline Γ_W, and a circular exterior boundary Γ_J. Within this region, the free suface is discretized into planar panels, and integration is performed numerically by means of a quadrature formula. Outside this region, a simplification is possible by exploiting vertical axisymmetry, which allows one to develop the first order potential and the Green function into Fourier series in the polar angle θ. After integration in the circumferential direction and use of orthogonality for each Fourier mode, the two dimensional free surface integral can be reduced to a series of one dimensional radial line integrals which can be integrated numerically. In order to speed up convergence, numerical quadrature is only employed up to a finite range but complemented by an analytic integration to infinity. Eventually, the integrand can be represented by summations of polynomials of various orders. Integration of each term of the polynomials satisfies a simple recurrence relationship from which its value can be easily calculated.

Theoretically, the free surface integrand appears relatively trouble free to obtain since it can be expressed as functions of the known first order solution. However, since the first order potential itself is obtained numerically, high accuracy of its second derivative is then very difficult to achieve. Moreover, it would be intuitively expected that the effect of the non-linearity in the free surface condition would be strongly concentrated in the immediate vicinity of the body. Hence special attention must be paid to efficient and accurate evaluation of this second derivative in the flow region around the body (e.g. in S_{Fi}). By use of integration by parts in two dimensions (or Green's Theorem), it is possible to express the integral containing the second derivative as one containing only the first order derivative plus two line integrals taken along the boundary of S_{Fi}.

To arrive at the one dimensional form of the free surface integral in the outer region, the first order velocity potential, and the Green's function, are

expressed as Fourier series in the polar angle θ. Based on eq. (1), where now C=1, this leads to

$$\phi^{(1)}(r,\theta,z) = \sum_{m=-\infty}^{\infty} \sum_{n=0}^{\infty} B_{mn} K_{mn}(\kappa_n r_0) Z_n(\kappa_n z_0) e^{im\theta_0} \qquad (15)$$

where the coefficients of the series, B_{mn}, are given by

$$B_{mn} = \frac{1}{2\pi} \int_{S_B} (V(\xi) - \phi^{(1)} \frac{\partial}{\partial n_\xi}) I_{mn}(\kappa_n r) Z_n(\kappa_n z) \cdot e^{-im\theta} dS_\xi \qquad (16)$$

Here I_m and K_m are modified Bessel functions of the first and second kind respectively; Z_n forms an orthonormal set of the vertical eigenfunctions for the linear free surface potential problem; and κ_n are the roots of the corresponding dispersion equation. Equation (16) is evaluated by numerical quadrature, after expressing $\phi^{(1)}$ on S_B in terms of the known nodal potentials and the shape functions.

The effective pressure term f in the free surface integral (c.f. eq. (9)) involves products of first order potentials. In the outer region the contribution from the evanescent modes n >> 1 can be ignored, and the integral itself therefore involves triple products of the n=0 terms (which in fact are more conveniently expressed as Hankel functions with real arguments). By substituting the leading terms for the related Hankel functions, the integrands may be approximated in a straightforward manner. The infinite integrals follow in the form of simple Fresnel integrals and can be evaluated explicitly. However, in this approach, the chosen value of R_J, which is the radius of the circular boundary Γ_J, has to be very large (especially for large m), so that the leading order approximation can yield sufficient accuracy for r greater than R_J. For smaller R_J, the leading order terms are not sufficiently accurate by themselves, but they can be amended by residual corrections, which have the form of asymptotic power series. In this manner, more refined approximations for the integrands can be obtained. One observes that the leading asymtotic does not depend on the order m; this order, however, appears in the coefficients of the full asymptotic expansions. In other words, the asymptotic series are not uniform with respect to m. An adaptive approach which not only overcomes this limitation but also ensures the accuracy of using Hankel's asymptotic expansions has been developed. Details of this have been given by Chau (1989), together wtih a criterion for selecting R_J and an extensive demonstration of convergence.

Within the inner free surface region S_{Fi} a numerical scheme has been employed based again on quadratic triangular or quadrilateral planar elements. The first order potential and its derivatives are obtained at the integration points by means of the shape functions. The integral involving second derivatives of $\phi^{(1)}$ on S_{Fi} is expressed in terms of first derivatives and line integrals on the boundary of the inner free surface region, as discussed above. The surface integrals are evaluated in a similar manner to those arising in the first order problem. The body waterline and the outer boundary of S_{Fi} are discretised by quadratic line elements, and the resulting line integrals are obtained by 3-point Gaussian adaptive quadrature.

5. NUMERICAL RESULTS

5.1 Vertical circular cylinders

In order to confirm the validity and accuracy of the numerical model, the case of second order diffraction by a vertical circular cylinder has been extensively investigated. The numerical results have been compared with those from analytical solutions. A solution for the distribution of second order potential on the cylindrical surface has been given by Eatock Taylor, Hung and Chau (1989) together with a discussion of the behaviour of $\phi_S^{(2)}$. A more general semi-analytical solution has also been obtained by Chau (1989), which provides the second order potential and flow kinematics associated with diffraction by the vertical cylinder, at any point in the fluid region. The two solutions are "exact", and therefore equivalent on the body surface. Results are here given for the same case as discussed in the previous section (i.e. a/d =1, ka =1.4). Due to the quadrupling effect on wave number by doubling the frequency, the levels of discretisation on the body surface used for the first order solution will no longer be sufficient for second order computation. In view of this, a finer discretisation (20 elements per quadrant) has been used to describe the body surface. The cylindrical mesh on the free surface is chosen to have an outer radius of 2d, and is discretised into 16 quadratic elements per quadrant. Typical comparisons down the vertical sides of the cylinder are shown in fig. 3 for two azimuthal angles θ. They are in good agreement, as can be seen from the results presented, except that just noticeable differences appear in the vicinity of the free surface.

As a separate exercise in validation, we have compared our results with the results of Kim and Yue (1989), which are based on a numerical analysis for axisymmetric bodies. Figure 4 shows a comparison betwee Kim and Yue's results and our analytical solution, for the second order run-up around a vertical circular cylinder in waves of amplitude A. The radius a of the cylinder equals the water depth, and the dimensionless frequency parameter $\omega^2 a/g = 2$. The first and second order quantities plotted are non-dimensionalised by A and A^2/a respectively. The solid line designates the total second order oscillatory component. Kim and Yue's results for this component are based on a discretisation of a generator of the cylinder by 20 segments, i.e. the use of 20 ring sources, each decomposed into 14 Fourier harmonics. The accuracy of these numerical results in relation to the analytical solution, appears comparable to those shown in fig. 3. Indeed this might be expected, since both numerical solutions use roughly similar numbers of unknowns in the discretisation. The results are also consistent with those obtained by the method of Scolan and Molin (1989).

5.2 Group of 4 cylinders

To demonstrate the use of the present method for a more realistic configuration in practice, a geometry comprising a group of cylinders is now investigated. This structure consists of four truncated vertical cylinders arranged on a square planform, typical of the columns of a TLP. The idealised case considered here is based on cylinders of radius 12.5m, and draft 37m, in water of depth 100m. The cylinders are placed at the corners of a square, of side 75m, and the unit amplitude incident wave propagates in a direction parallel to two sides of the square. This arrangement is the same as the four columns of the Snorre TLP

design. Local polar coordinates are defined such that the cylinder surfaces at θ=180° and at θ=270° are closest to the neighbouring cylinders, which are respectively in lines parallel and perpendicular to the direction of the incident wave.

As a check of the numerical model, two discretisations are employed to test the convergence of results (see fig. 5). A non-dimensional wave frequency of ka=0.5 is considered, corresponding to a wavelength of 157m (period=10s). Components of the horizontal and vertical diffraction forces for both the first and second order analyses are listed in table 2, showing comparisons between the numerical results obtained from mesh I (241 nodal points per column) and mesh II (1036 nodal points per column). It is evident that the results have converged. Local resolution of the flow such as the distribution of $|\phi_S^{(2)}|$ presents a more difficult problem than evaluation of global forces. In view of this, typical comparisons down the vertical sides of both the upwave and downwave cylinders are shown in fig. 6 for two azimuthal angles. They are in good agreement, as can be seen from the results presented, except that some differences are noticeable near the free surface. The closeness of the two sets of results suggests that for the conditions investigated, adequate accuracy can be obtained by using the relatively coarse mesh. Of course, finer discretisations are required for shorter waves.

In fig. 7, the magnitudes of the second order diffracted potential are plotted against the azimuthal angle on the waterlines of both the upwave and downwave cylinders. Numerical results for an isolated cylinder are also superimposed on the same diagram. One observes that the variation of $|\phi_S^{(2)}|$ along the waterline of the downwave cylinder has a trend very similar to the isolated member, except that local magnification (relative to the isolated cylinder) often occurs. This is particularly evident on the surface around θ=270°. Comparatively large values of $|\phi_S^{(2)}|$ are also observed at the weather side, suggesting that at second order there is little shielding from the upwave cylinders. In general, pronounced interaction effects can be seen along the circumference of the upwave cylinder. This is particularly interesting around θ=180° where the corresponding first order potential is much less sensitive to the existence of the neighbouring bodies.

Next results are presented in figure 8 showing isometric plots of second order free surface elevations. For the same 10s wave to which the results in fig. 7 relate, fig. 8a shows the instantaneous second order free surface elevation at the instant the incident wave of unit amplitude has a crest half way between upwave and downwave cylinders. Figure 8b shows the corresponding elevation one second later. There is strong evidence of the pronounced interactions arising from multiple scattering at second order between the columns.

5.3 Tension leg platforms

Results have also been obtained for a four column tension leg platform, based on the four cylinders described above. These were connected at the bottom by square pontoons of side 11.5m, such that the total platform draft remained 37.5m. The mesh of quadratic isoparametric elements used to discretise the TLP is shown in fig. 9. The instantaneous free surface elevation corresponding to a 10s wave of unit amplitude is shown in fig. 10. This may be compared directly with fig. 8a, from which it appears that the effect of the pontoons on the second order upwelling phenomenon is in fact rather small. This behaviour can be inferred from simpler analyses of bottom mounted and truncated single cylinders. By comparing such analyses, one finds that the behaviour of the second order diffacted potential on the free surface is in general not sensitive to the presence or absence of structural members located at large depth of submergence. Moreover, this effect becomes more pronounced at higher frequencies.

6 CONCLUDING REMARKS

Some of the conclusions from the investigation summarised above are the following.

1) Reliable solution of the second order diffraction problem requires accurate numerical analysis of the linear problem. An effective way of achieving this has been found to be the use of quadratic isoparametric boundary elements. These have been used to discretise a modified integral equation, which reduces the effect of the singularity in the dipole distribution. Further benefit in treating the singularities has been gained from use of a special triangular coordinate transformation. Extremely accurate first order results have been obtained using very few elements.

2) It is necessary to exercise considerable care in evaluating the free surface integral which appears in the formulation of the second order problem. A highly effective approach has been found to be the use of Hankel's asymptotic series for various terms in the integrand.

3) Substantial efforts have been made to validate the methods and programs used here, and rapid convergence to the few available analytical solutions has been observed. There is, however, a need for some widely agreed benchmarks. Even simple geometries, such as floating truncated cylinders, can provide challenging problems in terms of convergence (e.g for results associated with the pitch mode). Suitable cases suggested at the FPS 2000 discussions (Nielsen et al. 1990), included truncated cylinders of radius to draft ratios 0.125, 1.0, 4.0 in a water depth of 10 radii. Analysis of these cases is currently in hand.

4) The importance of second order diffraction effects has been reaffirmed in this investigation, for a range of relevant parameters. A crucial difference in the behaviour of first and second order forces is the very slow decay of the latter with increase in water depth. This feature may have a significant effect on the design of deep draft floaters. The vertical force on a truncated cylinder due to the second order potential has been found to be much greater than the second order vertical force resulting from first order potentials. This is of extreme importance to the prediction of vertical resonant motions in deep water TLP's.

ACKNOWLEDGEMENTS

This work was supported by the Croucher Foundation (Hong Kong) and the Managed Programme on Floating Production Systems (jointly funded by SERC and industry through the Marine Technology Directorate Ltd).

REFERENCES

Breit, S.R., Newman, J.N. and Sclavounos, P.D. 1985, "A new generation of panel programs for radiation-diffraction problems". Proc. 4th Int. BOSS Conf., Delft, Elsevier, 531-544.

Chau, F.P., 1989, "The second order velocity potential for diffraction of waves by fixed offshore structures", Thesis for the Ph.D. degree in the University of London, University College London.

Chau, F.P. and Eatock Taylor R., 1988, "Second order velocity potential for arbitrary bodies in waves", Proc. 3rd Int. Workshop on Water Waves and Floating Bodies, Woods Hole, 15-19.

Eatock Taylor, R., Hung S.M. and Chau, F.P., 1989, " On the distribution of second order pressure on a vertical circular cylinder", Applied Ocean Research 11, 183-193.

Eatock Taylor, R., and Jefferys, E.R., 1986, "Variability of hydrodynamic load predictions for a tension leg platform", Ocean Engineering 13, 449-490.

Eatock Taylor, R. and Zietsman, J., 1982, "Hydrodynamic loading on multicomponent bodies", Proc. 3rd Int. BOSS Conf., MIT, Hemisphere Publishing Corp., Vol 1, 424-443.

Hess, J.L. and Smith, A.M.O., 1964, "Calculation of non-lifting potential flow about arbitrary three dimensional bodies", J. Ship Res. 8, 22-44.

Hogben, N. and Standing R.G., 1974, "Wave loads on large bodies", Proc. Int. Symp. Dynamics of Marine Vehicles and Structures in Waves, Inst. Mech. Eng. London.

Kim, M.H. and Yue, D.K.P., 1989, "The complete second order diffraction solution for an axisymmetric body. Part 1, monochromatic waves", J. Fluid Mech. 200, 235-264.

Korsmeyer, F.T., Lee, C.H, Newman, J.N. and Sclavounos, P.D., 1988, "The analysis of wave effects on tension leg platforms", Proc. 7th Offshore Mech. and Arctic Eng. Conf., Houston 2, 1-20.

Li, H.B., Han, G.M. and Mang, H.A., 1985, "A new method for evaluating singular integrals in stress analysis of solids by the direct boundary element method", Int. J. Num. Mech. Eng. 21, 2071.

Liu, Y.H., 1988, "Analysis of fluid structure interaction by using higher order boundary elements in potential problems and its application in coupling vibrations in bending and torsion of ships", Thesis for the Ph.D. degree in Shanghai Jiao Tong University.

Liu, Y.H., Kim, C.H. and Lu, X.S., 1990, "Comparison of higher order boundary element and constant panel methods for hydrodynamic loading", Proc. EUROMS, Stavanger.

Newman, J.N. and Sclavounos, P.D., 1988, "The computation of wave loads on large offshore structures", Proc.5th Int. BOSS Conf., Trondheim, Tapir 2, 605-622.

Nielsen, F.G., Herfjord, K. and Loken A., 1990, "Floating production systems in waves. Results from a comparative study on hydrodynamic coefficients, wave forces and motion responses", FPS 2000, NTNF Report.

Noblesse, F., 1988, "Integral identities of potential theory of radiation and diffraction of regular waves by a body", J. Eng. Math. 17, 1-3.

Noblesse, F. and Hendrix, D., 1990, "Fourier-Kochin representation of the flow due to a ship advancing in regular waves", Proc. IUTAM Symp. Dynamics of Marine Vehicles and Structures in Waves, Brunel University.

Scolan, Y.M. and Molin, B., 1989, "Second order deformation of the free-surface around a vertical cylinder", Proc. 4th Workshop on Water Waves and Floating Bodies, Oystese 227-232.

Wu, G.X. and Eatock Taylor, R., 1989, "The numerical solution of the motions of a ship advancing in waves", Proc 5th Int. Conf. Num. Ship Hydrodyn., Hiroshima 386-394.

z/d	θ^o	analytical solution	numerical solution mesh I	mesh II
0.0	0	(-0.1788E+1, 0.2572E+1)	(-0.1788E+1, 0.2571E+1)	(-0.1788E+1, 0.2572E+1)
0.0	45	(-0.7715E+0, 0.1144E+1)	(-0.7651E+0, 0.1143E+1)	(-0.7709E+0, 0.1144E+1)
0.0	90	(-0.7104E+0, -0.9172E+0)	(-0.6988E+0, -0.9135E+0)	(-0.7096E+0, -0.9168E+0)
0.0	135	(-0.1878E+1, -0.1906E+0)	(-0.1871E+1, -0.1853E+0)	(-0.1878E+1, -0.1898E+0)
0.0	180	(-0.2090E+1, 0.7424E+0)	(-0.2087E+1, 0.7482E+0)	(-0.2090E+1, 0.7433E+0)
-1.0	0	(-0.8312E+0, 0.1196E+1)	(-0.8348E+0, 0.1196E+1)	(-0.8315E+0, 0.1196E+1)
-1.0	45	(-0.3587E+0, 0.5317E+0)	(-0.3588E+0, 0.5319E+0)	(-0.3587E+0, 0.5317E+0)
-1.0	90	(-0.3303E+0, -0.4264E+0)	(-0.3266E+0, -0.4249E+0)	(-0.3300E+0, -0.4263E+0)
-1.0	135	(-0.8732E+0, -0.8859E-1)	(-0.8722E+0, -0.8785E-1)	(-0.8731E+0, -0.8850E-1)
-1.0	180	(-0.9716E+0, 0.3452E+0)	(-0.9737E+0, 0.3458E+0)	(-0.9717E+0, 0.3452E+0)

Table 1 Distribution of $\phi_s^{(1)}$ on the surface of a vertical circular cylinder (real and imaginary parts)

mesh	1st order diffraction force		2nd order diffraction force	
	horizontal	vertical	horizontal	vertical
I	3.46E+06	7.50E+05	7.29E+05	3.46E+05
II	3.46E+06	7.46E+05	7.33E+05	3.45E+05

Table 2 Magnitude of the first and second order diffraction forces on four truncated vertical cylinders (in Newtons)

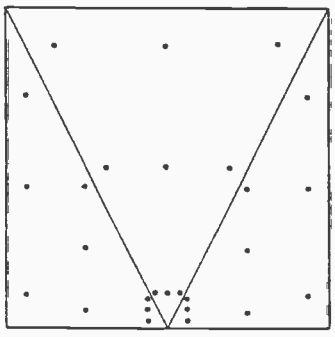

Fig 1. Distribution of integration points

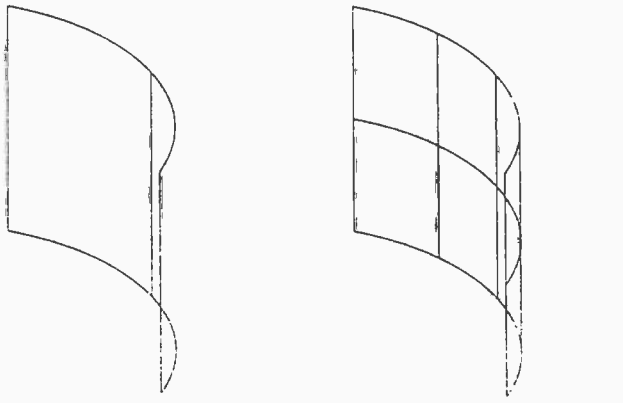

(a) mesh I
2 elements per quadrant

(b) mesh II
8 elements per quadrant

Fig 2. Different levels of discretisation on the body surface of a vertical circular cylinder

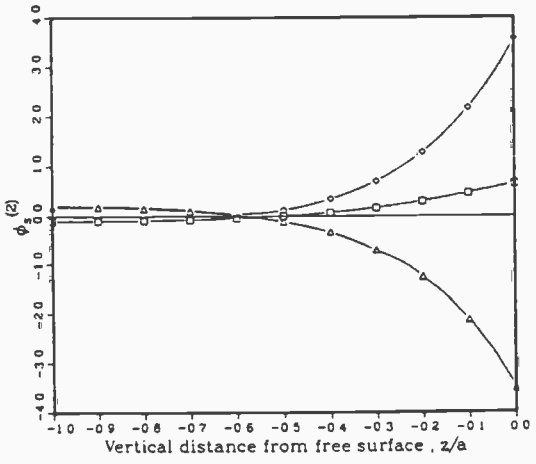

(a) θ=0°

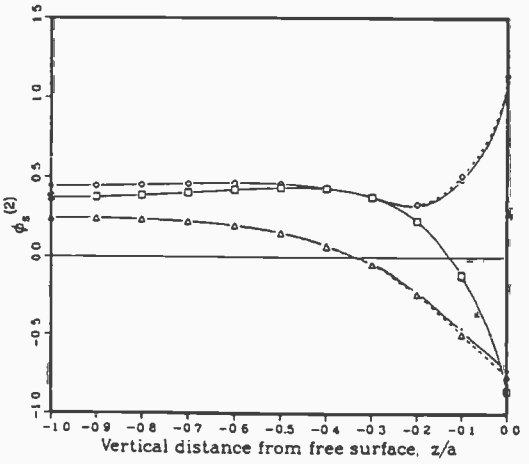

(b) θ=90°

Fig 3. Distribution of $\phi_s^{(2)}$ along the sides of a vertical cylinder: o Re $[\phi_s^{(2)}]$; ▽ Im $[\phi_s^{(2)}]$; ◇ $|\phi_s^{(2)}|$; ----- direct method; _____ numerical method

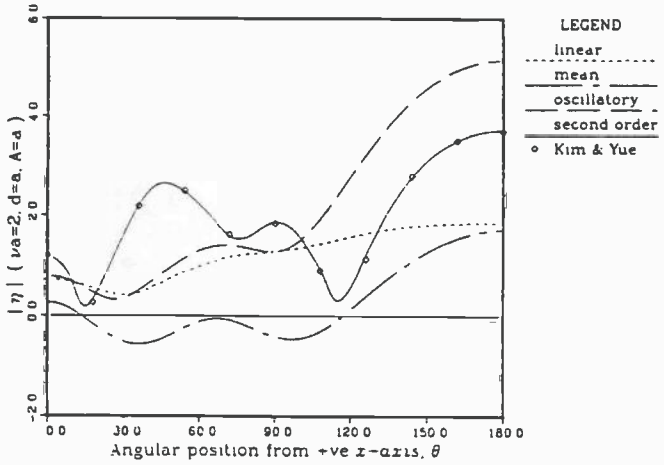

Fig 4. Linear and second order components of run up around a vertical cylinder

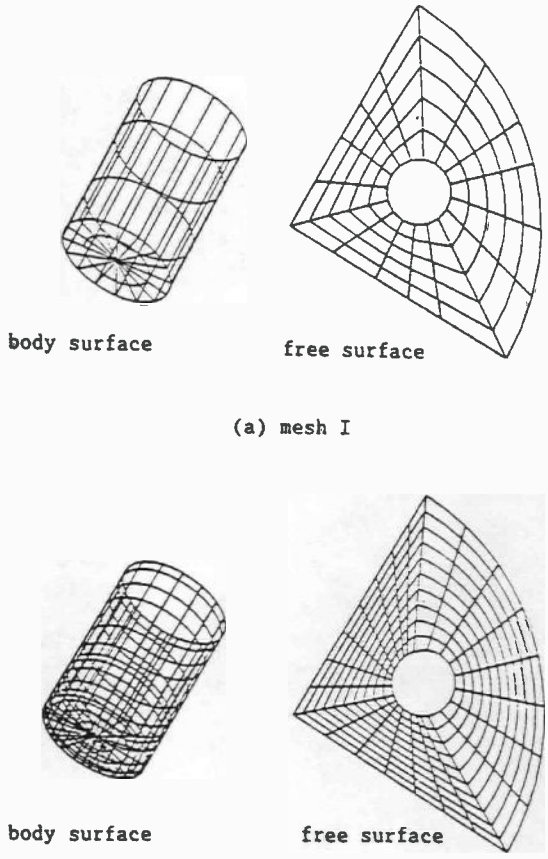

Fig 5. Discretisations of body surface and free surface for group of four truncated vertical cylinders (with two planes of symmetry)

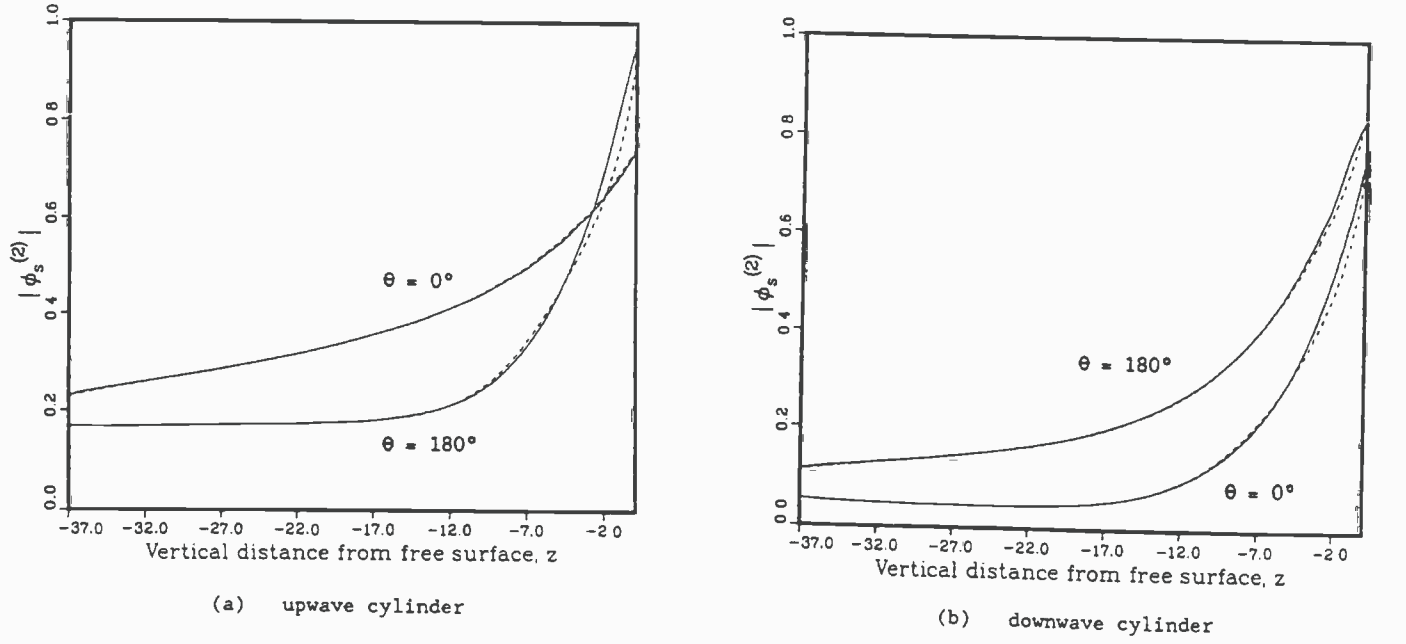

Fig 6. Comparison of the vertical distribution of $|\phi_s^{(2)}|$ for two different meshes: ---- mesh I; —— mesh II

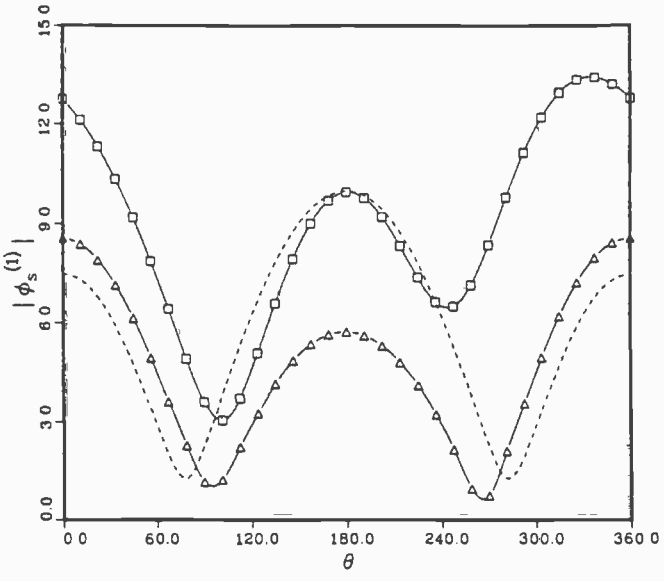

Fig.7 Distributions of $|\phi_s^{(2)}|$ along the waterlines of four truncated vertical cylinders:

--- isolated cylinders;
-o- upwave cylinder;
-Δ- downwave cylinder.

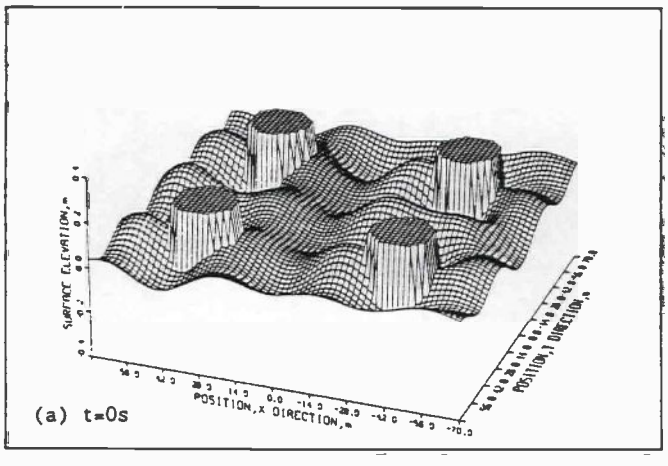

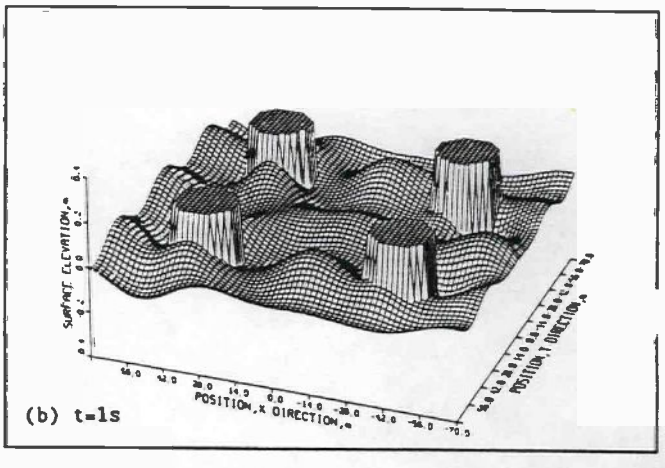

Fig 8. Isometrics of the second order free surface profile due to $\phi_s^{(2)}$ for a 10s wave diffracted by four truncated vertical cylinder:

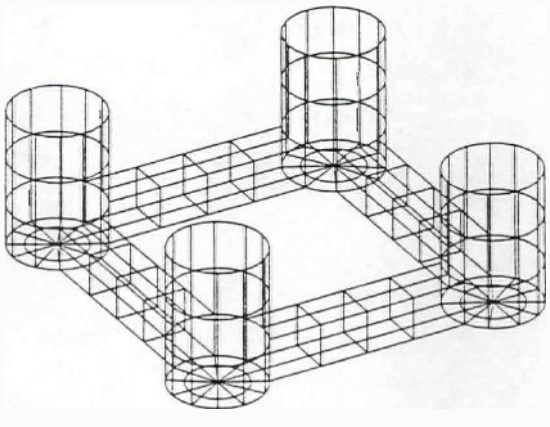

Fig 9. Discretisation of the submerged surface of a TLP by quadratic isoparametric elements

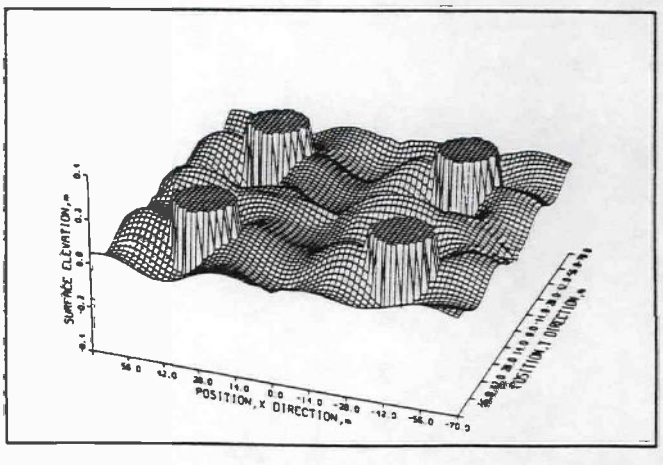

Fig 10. Isometric of the second order free surface profile due to $\phi_s^{(2)}$ for a 10s wave diffracted by a TLP